Functional validation of tensin2 SH2-PTB domain by CRISPR/Cas9-mediated genome editing

Kiyoma MARUSUGI[1)], Kenta NAKANO[1,2)], Hayato SASAKI[1)], Junpei KIMURA[4)], Rieko YANOBU-TAKANASHI[2,3)], Tadashi OKAMURA[2,3)] and Nobuya SASAKI[1)]*

[1)]*Laboratory of Laboratory Animal Science and Medicine, School of Veterinary Medicine, Kitasato University, Towada, Aomori 034-8628, Japan*

[2)]*Department of Laboratory Animal Medicine, Research Institute, National Center for Global Health and Medicine, Tokyo 162–8655, Japan*

[3)]*Department of Infectious Diseases, Section of Animal Models, Research Institute, National Center for Global Health and Medicine, Tokyo 162–8655, Japan*

[4)]*Laboratory of Anatomy, Department of Biomedical Sciences, Graduate School of Veterinary Medicine, Hokkaido University, Sapporo, Hokkaido 060–0818, Japan*

ABSTRACT.   Podocytes are terminally differentiated and highly specialized cells in the glomerulus, and they form a crucial component of the glomerular filtration barrier. The ICGN mouse is a model of glomerular dysfunction that shows gross morphological changes in the podocyte foot process, accompanied by proteinuria. Previously, we demonstrated that proteinuria in ICR-derived glomerulonephritis mouse ICGN mice might be caused by a deletion mutation in the tensin2 (*Tns2*) gene (designated *Tns2nph*). To test whether this mutation causes the mutant phenotype, we created knockout (KO) mice carrying a Tns2 protein deletion in the C-terminal Src homology and phosphotyrosine binding (SH2-PTB) domains (designated *Tns2ΔC*) via CRISPR/Cas9-mediated genome editing. *Tns2nph*/*Tns2ΔC* compound heterozygotes and *Tns2ΔC*/*Tns2ΔC* homozygous KO mice displayed podocyte abnormalities and massive proteinuria similar to ICGN mice, indicating that these two mutations are allelic. Further, this result suggests that the SH2-PTB domain of Tns2 is required for podocyte integrity. *Tns2* knockdown in a mouse podocyte cell line significantly enhanced actin stress fiber formation and cell migration. Thus, this study provides evidence that alteration of actin remodeling resulting from Tns2 deficiency causes morphological changes in podocytes and subsequent proteinuria.

KEY WORDS: CRISPR/Cas9, glomerular sclerosis, podocyte, SH2-PTB domain, tensin2

doi: 10.1292/jvms.16-0205; *J. Vet. Med. Sci.* 78(9): 1413–1420, 2016

Glomerular podocytes are highly specialized cells with a complex cytoarchitecture. Their most prominent features are interdigitated foot processes (FP) with filtration slits. These are bridged by the slit diaphragm, which plays a major role in establishing the selective permeability of the glomerular filtration barrier. Injury to podocytes leads to proteinuria, a hallmark of most glomerular diseases [30].

The ICGN mouse is a model of glomerular sclerosis (GS) that shows gross morphological changes in the podocyte FP, accompanied by proteinuria. The ICGN mouse is also a model of chronic kidney disease (CKD) that presents the common symptoms and pathological changes associated with a variety of kidney diseases, such as hypoproteinemia, hyperlipidemia, anemia and systemic edema, and eventual end-stage renal failure [28, 29]. Previously, we identified a major quantitative trait locus (QTL) on chromosome 15 that is identical to a single recessive locus causing proteinuria, and found a deletion mutation in the tensin2 (*Tns2*) gene (designated *Tns2nph*). The deletion consists of 8 nucleotides situated in exon 18 of *Tns2*, causing a frameshift and a premature termination codon [6]. The truncated transcript also shows decreased expression, probably due to nonsense-mediated mRNA decay; the intrinsic expression site of Tns2 is the healthy kidney.

Tensins (Tns) comprise a family of multidomain scaffold proteins that bind the cytoplasmic tail of β integrins, and localize to adhesions that anchor stress fibers in cells; they are thought to be an important component linking the extracellular matrix, the actin cytoskeleton and signal transduction [19]. In addition, *Tns2* is highly expressed in podocytes [6], and *Tns2* deficiency is thought to alter podocyte function/cytoarchitecture, resulting in GS in ICGN mice. However, because Tns3 is also highly expressed in the glomeruli and shows a high level of sequence similarity to Tns2, Tns3 is thought to be able to compensate for the absence of Tns2 [26]. Further, since this QTL region is very broad, it may contain other causative genes associated with the development of GS in ICGN mice. To date, there is no genetic evidence that Tns2 deficiency alone is sufficient to cause GS in ICGN mice.

Tns2 is a multidomain protein composed of a PKC-C1/

PTPase domain at the N-terminus followed by a PTEN region and a Src homology 2 (SH2)/phosphotyrosine binding (PTB) domain at the C-terminus [19]. The SH2-PTB domain has been suggested to bind to the intracellular domain of integrin-family proteins, resulting in intracellular transmission of the integrin signal, leading to adjustment of cytoskeleton dynamics [3, 5]. However, little is known about the function of the SH2-PTB domain *in vivo*.

RNA-guided, nuclease-mediated genome editing, based on the CRISPR/Cas system, offers an efficient and convenient technique for genome editing [14]. In brief, Cas9, a nuclease guided by single-guide RNA (sgRNA), binds to a targeted genomic sequence next to the protospacer adjacent motif (PAM) and generates a double-strand break (DSB). The DSB is then repaired by nonhomologous end-joining (NHEJ), leading to insertion/deletion mutations [20].

To test whether Tns2 mutation might cause the GS phenotype and to clarify the biological role of the SH2-PTB domain, we created knockout mice carrying a Tns2 protein deletion in the SH2-PTB domain via CRISPR/Cas9-mediated mutagenesis.

MATERIALS AND METHODS

Ethical statement: All research was conducted according to the Regulations for the Care and Use of Laboratory Animals of Kitasato University and the National Center for Global Health and Medicine. The animal experimentation protocol was approved by the President of Kitasato University based on the judgment of the Institutional Animal Care and Use Committee of Kitasato University (Approval ID: No. 15–053). A humane end point was applied when mice with severe anemia became moribund.

Mouse: CRISPR/Cas9-mediated genome editing in mice was performed as described previously [27]. Briefly, sgRNA expression vector for the target sequence (AGAGA-CAGCCATTCATTCCA) coupled with a T7 promoter was synthesized (Eurofins Genomics, Brussels, Belgium), and transcribed *in vitro* using the MEGAshortscript kit (Thermo Fisher Scientific, Waltham, MA, U.S.A.). *hCas9* mRNA from pX330 (https://www.addgene.org/42230/) was synthesized using the mMESSAGE mMACHINE T7 kit (Thermo Fisher Scientific) and was polyadenylated with the Poly (A) Tailing kit (Thermo Fisher Scientific). The purified *hCas9* mRNAs (100 $ng/\mu l$) and sgRNAs (50 $ng/\mu l$) were co-injected into the cytoplasm of fertilized eggs derived from BDF1 females (Japan SLC, Hamamatsu, Japan). After the injected oocytes were cultured overnight *in vitro*, two-cell embryos were transferred into pseudo-pregnant female mice. Genomic DNA was isolated from the offspring from samples taken from the tail, using standard methods. The region around exon 22 of the *Tns2* locus was amplified by PCR, using two sets of primers: Tns2 forward, GCCTCAGACTA-AATGTTGTTCCAAGT and Tns2 reverse, GAAATGGCG-GACCAGCTGTTCTGA. The amplification products were sequenced and compared to the wild-type. The resulting founder animals were crossed to FVB/N mice (CLEA Japan, Tokyo, Japan) and then backcrossed to the same for three

generations. The *Tns2^{AC}* KO heterozygote mice were bred to *Tns2^{AC}* KO heterozygote and *Tns2^{nph}* (FVB-*Tns2^{nph}*) mice to produce compound heterozygotes (*Tns2^{nph}/Tns2^{AC}*) and homozygous knockouts (*Tns2^{AC}/Tns2^{AC}*), respectively. The *nph* genotype derived from the original ICGN mice was determined as described previously [32].

Measurement of urinary albumin excretion: Urine samples were collected by gentle manual compression of the abdomen. A 10- μl aliquot [containing 2% SDS, 5% β-mercaptoethanol, 10% glycerol, 60 mM Tris-HCl (pH 6.8), bromophenol blue and 5 μl of urine] was heated for 5 min at 95°C and subjected to 10% SDS-polyacrylamide gel electrophoresis. As a positive control, bovine serum albumin (BSA) was loaded simultaneously. The gel was fixed and stained with Coomassie brilliant blue (CBB; Wako, Osaka, Japan) according to the manufacturer's instructions. CBB-stained urinary albumin was quantified using the image analysis program ImageJ (http://rsb.info.nih.gov/ij/).

Histology: Ten-week-old mice were sacrificed by an overdose of isoflurane, and whole kidneys were dissected out. The kidneys were embedded in OCT compound and frozen with liquid nitrogen. Four-micrometer-thick cryostat sections were cut, transferred to MAS-coated slides, air dried and stored at −80°C until use. For immunohistochemical analysis, the slides were washed in PBS, fixed with acetone at 4°C and incubated for 8 hr at 4°C with the primary antibody diluted in 1% BSA in PBS [rabbit anti-Tns2 central portion [26] 1:1,000; and rabbit anti-Tns2 C-terminal (SAB4200268, Sigma-Aldrich, MO, U.S.A.) 1:1,000]. The slides were then washed in PBS and incubated with biotin-conjugated donkey anti-rabbit IgG as a secondary antibody (Histofine; Nichirei Biosciences, Tokyo, Japan) for 30 min at room temperature and treated with horseradish peroxidase-conjugated streptavidin complex (Histofine; Nichirei Biosciences) for 3,3-diaminobenzidine staining. Lastly, slides were dehydrated and mounted. Periodic acid-Schiff (PAS) staining and ultrastructural analysis were performed using transmission electron microscopy (TEM) as described in our previous report [32].

Knockdown of Tns2 in the podocyte cell line: The conditionally immortalized mouse podocyte cell line MPC5 used in our study was a kind gift from Professor Peter Mundel [25]. Briefly, the podocytes were cultured at 33°C in RPMI1640 medium (Thermo Fisher Scientific) containing 10% fetal bovine serum (Thermo Fisher Scientific) and 100 U/m*l* recombinant mouse interferon-γ (Sigma-Aldrich). MPC5 cells were inoculated at a density of 5×10^5 cells/well in 6-well plates. After 24 hr, cells at 70–80% confluence were transfected with Stealth Select RNAi (CCACUCAAAGCAACGCAGUA-CUCUA, UAGAGUACUGCGUUGCUUUGAGUGG, MSS209763, Thermo Fisher Scientific) (nucleotides 321–345 of *Tns2* cDNA; Accession no. NM_153533.2) or MISSION siRNA universal negative control (Sigma-Aldrich) in serum-free medium using lipofectamine 3000 (Thermo Fisher Scientific) according to the manufacturer's instructions. To differentiate MPC5 cells after siRNA transfection, the cells were plated on type I collagen dishes and cultured with 1% FBS in a 5% CO_2 atmosphere at 37°C for 3 days. To confirm silenc-
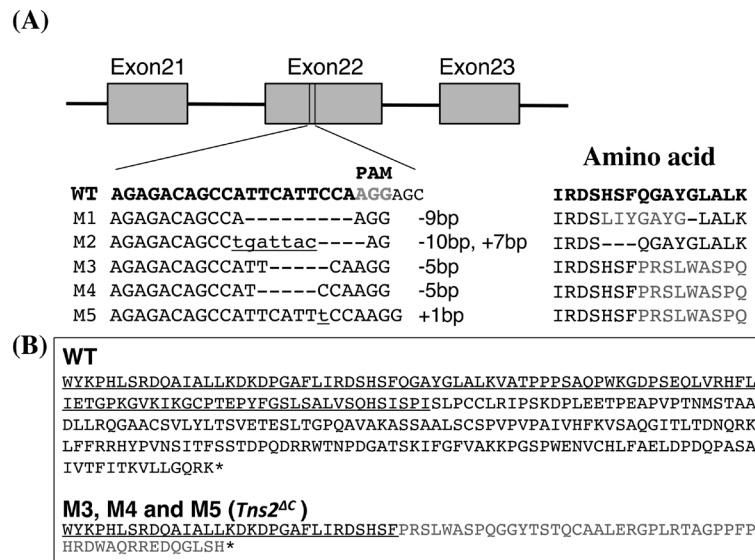
(A)

(B)

Fig. 1. Generation of *Tns2*-modified mice using the CRISPR/Cas9 system. (A) PCR amplicons of the targeted fragment in *Tensin2* (*Tns2*) in founder mice were sequenced. The target sites of the sgRNA are shown in bold font; the PAM sequence is highlighted in grey; the insertional mutations are underlined and in lower case; insertions (+) or deletions (−) are shown to the right of each allele. Substitutions or deletions of amino acid residues are highlighted in grey. (B) Tns2 amino acid sequences. The upper sequence is the amino acid sequence of WT mice, and the lower is the SH2-PTB domain deletion sequence of the M3, M4 and M5 founders. The common sequence is underlined. The frame-shift mutation identified in M3, M4 and M5 mice is shown in gray font; it led to changes in the amino acid sequence of the SH2 domain and loss of the entire PTB domain.

ing of *Tns2* expression, quantitation of *Tns2* (NM_153533.2) and *Gapdh* (NM_001289726.1) expression was performed by quantitative RT-qPCR. Total RNA was extracted from MPC5 cells using the RNeasy mini kit (Qiagen, Hilden, Germany) at 72 hr post-transfection. One microgram of total RNA was used for cDNA synthesis with ReverTra Ace (Toyobo, Osaka, Japan) and oligo dT primers. RT-qPCR was performed using the KAPA SYBR Fast qPCR Kit (Kapa Biosystems, Wilmington, MA, U.S.A.) according to the manufacturer's instructions. The reactions were analyzed using the Illumina Eco Real-Time PCR System (Illumina, San Diego, CA, U.S.A.). Primers were designed for *Tns2* (AAAGGCGACGTCATG-GTAAC and CTCCACTGAGGCTTGGAAAG) and *Gapdh* (CGACTTCAACAGCAACTC and GCCGTATTCATTGT-CATACCAG). The results were normalized against *Gapdh* expression.

Cell Adhesion assay: Adhesion assays with crystal violet staining were performed according to the method described in a previous report [10]. *Tns2* knockdown (KD) MPC5 cells and control cells were trypsinized and seeded on 6-well plates coated with collagen type IV (Sigma-Aldrich, 10 mg/m*l*), laminin (Sigma-Aldrich, 10 mg/m*l*), vitronectin (Sigma-Aldrich, 10 mg/m*l*) or fibronectin (Sigma-Aldrich, 10 mg/m*l*) at a density of 1.5×10^4 cells per well. After incubation for 1 hr at 37°C, non-adherent cells were removed by gentle washing with PBS, followed by fixation in 100% ethanol. Cells were stained in 0.1% crystal violet for 15 min at 25°C, washed in water and then counted under a microscope. All experiments were performed in triplicate wells for each condition, and data are expressed as means ± standard deviation.

Statistical analyses were performed using Student's *t*-test and Dunn's multiple comparison test. *P*-values<0.05 were considered significant.

Transwell migration assays: *Tns2* KD MPC5 cells and control cells were plated in 8.0-*μ*m pore size transwell inserts at a density of 1.5×10^4 cells per well according to the method described in a previous report [13]. After 24 hr, the cells on the upper side of the insert were removed by scraping, and the cells that had migrated through were fixed on the lower side of the membrane with 100% ethanol, stained with crystal violet and quantified by counting the number of cells in 20 separate fields. All experiments were performed in triplicate wells for each condition, and the data are expressed as means ± standard deviation. Statistical significance was determined using Dunn's multiple comparison test, with *P*-values <0.05 considered significant.

Phalloidin staining of Tns2 KD cells: *Tns2* KD MPC5 cells and control cells were seeded onto 24-well collagen I-coated culture glass. To observe actin reorganization, wound gaps were made in the MPC5 monolayers by scratching using a 200-*μl* tip. Images were captured after 8 hr. Cells were rinsed twice with PBS, fixed with fresh methanol-free 3.7% PFA for 10 min, permeabilized with 0.1% Triton-X for 5 min and incubated with Alexa Fluor 594 Phalloidin (Thermo Fisher Scientific). Actin stress fibers were identified and quantified using the EVOS FL cell imaging system (Thermo Fisher Scientific). All experiments were performed in quintuplicate wells for each condition. Data are expressed as means ± standard deviation. Statistical significance was determined using Dunn's multiple comparison test, and *P*-
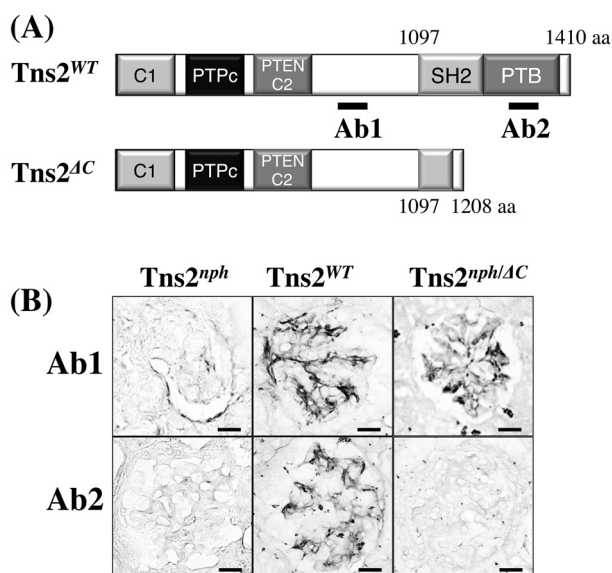
(A)

(B)

Fig. 2. Immunohistochemical analysis of Tns2 expression in the glomeruli of *Tns2^nph^*, *Tns2^WT^* and *Tns2^ΔC^* mice. (A) Functional and structural domains of Tns2. The upper domain is *Tns2^WT^* and the lower is *Tns2^ΔC^*, which lacks the putative SH2-PTB domain. C1, protein kinase C conserved region 1 domain; PTPc, protein tyrosine phosphatase catalytic domain; PTEN C2, C2 domain of PTEN tumor-suppressor protein; SH2, Src homology 2 domain; PTB, phospho tyrosine binding. (B) Immunohistochemical analysis of Tns2 expression in the glomeruli of *Tns2^nph^*, *Tns2^WT^* and *Tns2^nph/ΔC^* mice. Two antibodies (Ab1 and Ab2, shown by the black bars in Fig. 2A) recognize the central portion of Tns2 and the PTB domain, respectively. Both Abs detected Tns2 expression in the glomeruli of *Tns2^WT^* mice, but Tns2 protein expression was lost in *nph* homozygotes (*Tns2^nph/nph^*). In compound heterozygotes (*Tns2^nph/ΔC^*), Tns2 could be detected only by Ab1 but not by Ab2, indicating that the SH2-PTB domain had been deleted. Scale bars=10 μm.

values<0.05 were considered significant.

RESULTS

Generation of Tns2 SH2-PTB domain-KO mice: To generate mice carrying mutations that disrupt the Tns2 C-terminal SH2-PTB domain, we designed a sgRNA targeting exon 22 of *Tns2*. Exon 22 encodes the latter half of SH2, which binds specifically to many intracellular signal-transducing proteins (Fig. 1A). To verify genetic modification at the target locus, a region of genomic DNA including *Tns2* exon 22 was amplified by PCR and subjected to sequencing analysis. After co-microinjection of sgRNA/Cas9 mRNA into fertilized eggs, five types of progeny were born (Fig. 1A, founder mouse nos. M1–M5). M3, M4 and M5 mice had 5-bp deletions or a 1-bp insertion close to the PAM sequence, which might lead to frame-shift mutations and subsequent protein deletion in both the SH2 and PTB domains (designated as *Tns2^ΔC^*). All nucleotide changes in these mice were transmitted to the next generation by mating with the FVB strain.

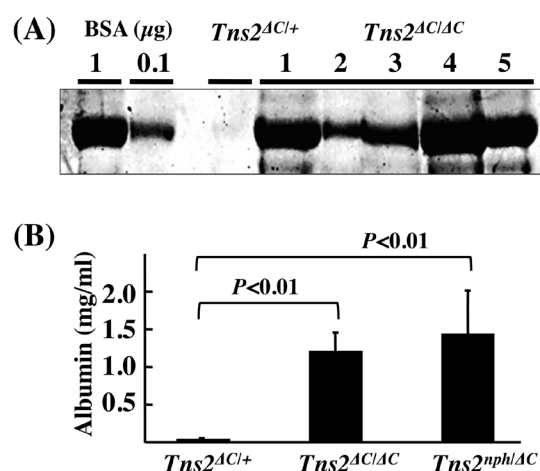*Loss of Tns2 results in proteinuria and FP effacement of*

(A)

(B)

Fig. 3. Measurement of albuminuria in *Tns2^ΔC^*-knockout mice. (A) SDS-PAGE analysis of representative individuals of heterozygote *Tns2^ΔC/+^* and homozygote *Tns2^ΔC/ΔC^* mice. Albumin bands (66 kDa) were observed in homozygous (nos. 1–5) mice from 4 weeks of age, but not in heterozygote (*Tns2^ΔC/+^*) mice. (B) CBB-stained urinary albumin was quantified using the image analysis program ImageJ. *Tns2^ΔC/ΔC^* (4 weeks of age, n=5), *Tns2^nph/ΔC^* mice (10 weeks of age, n=3) and *Tns2^WT^* (10 weeks of age, n=3) mice were used.

podocytes: Because the original ICGN mouse is a spontaneous mutant derived from a closed colony of ICR mice, there is no control strain. The FVB/N strain has been identified as susceptible to the development of GS and CKD [33]. Thus, we previously created FVB.ICGN-*Tns2^nph^* (FVB-*Tns2^nph^*) congenic mice. Next, genetic complementation testing was undertaken using FVB-*Tns2^ΔC^* and FVB-*Tns2^nph^*. *Tns2^ΔC^* heterozygous mice (M3 strain) were bred to *Tns2^nph^* homozygotes to produce compound heterozygotes (*Tns2^nph^/Tns2^ΔC^*) in the FVB strain background. To determine whether expression of the Tns2 protein remained at a normal level and only the SH2-PTB domain had been deleted, we conducted immunohistochemical analyses on kidney sections of compound heterozygotes (*Tns2^nph^/Tns2^ΔC^*) compared with FVB-*Tns2^nph^* homozygotes and age-matched wild-type (WT) controls (*Tns2^WT^/Tns2^WT^*). We used two antibodies recognizing the central portion of Tns2 and the C-terminal PTB domain, respectively (Fig. 2A). The use of the two antibodies revealed that Tns2 protein expression was lost in FVB-*Tns2^nph^* mice, which is in agreement with an earlier report [35]. In contrast, Tns2 protein expression and localization in glomeruli was normal in the compound heterozygotes. However, Tns2 could be detected by Ab1 but not by Ab2, indicating that the SH2-PTB domain had been deleted; deletion of this domain does not affect Tns2 protein stability (Fig. 2B).

In the compound heterozygotes, proteinuria was detectable at 4 weeks of age using SDS-PAGE, and subsequent CBB staining demonstrated remarkable proteinuria (Fig. 3B). In contrast, no urinary albumin excretion was detectable in FVB-*Tns2^ΔC/+^* mice (Fig. 3A and 3B). Histological analy-
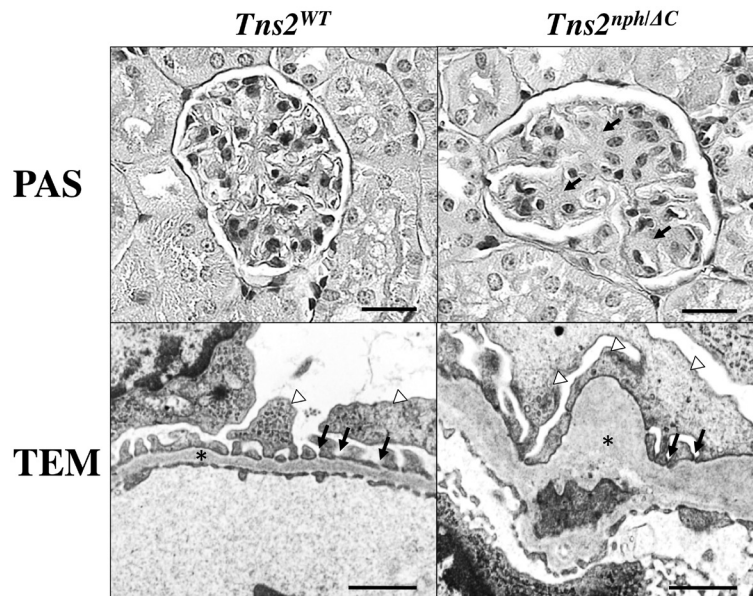
Fig. 4.   Renal histopathology of offspring. Representative light microscopy images with PAS staining (upper panel) of the kidney from $Tns2^{WT}$ mice (left) and $Tns2^{nph/\Delta C}$ (right) mice at 12 weeks of age. Black arrow: mesangial matrix. Scale bars=10 μm. TEM analysis (lower panel) of $Tns2^{WT}$ mice (left) and $Tns2^{nph/\Delta C}$ (right) mice at 12 weeks of age. *: GBM. Black arrow: slit diaphragm. White arrowhead: podocytes. Scale bar=1 μm.

sis with PAS staining revealed that almost all glomeruli in the compound heterozygote mice showed entire expansion of the mesangial matrix at 12 weeks of age (Fig. 4, upper panel). Ultrastructural analysis revealed fused podocyte FPs, loss of slit diaphragms and GBM thickening in all glomeruli in the compound heterozygotes at 12 weeks of age (Fig. 4, lower panel). In addition, homozygous $Tns2^{\Delta C}/Tns2^{\Delta C}$ mice displayed massive proteinuria similar to that seen in ICGN mice (Fig. 3B). In contrast, compound heterozygotes derived from M1 and M2 founders did not show any abnormalities (data not shown). Thus, the $Tns2^{nph}$ mutation was confirmed to be responsible for GS in ICGN mice. Further, this result suggests that the SH2-PTB domain of Tns2 is required for podocyte integrity. In addition, $Tns2^{\Delta C}$ homozygote mice did not show any of these other phenotypes, indicating a selective role for Tns2 in kidney function.

Loss of podocyte Tns2 results in increases in the formation of actin stress fibers and cell migration: Cell-cell contact and adherence of podocytes to the extracellular matrix of the GBM are crucial for podocyte function. It is well known that cell-to-cell and cell-to-extracellular matrix (ECM) adhesions affect morphological changes involved in cell migration. Integrins, a large family of cell adhesion proteins, mediate the adhesion of cells to the ECM and provide traction for cell motility. Many proteins present on the cytoplasmic side of focal adhesions, including those in the tensin family, are considered to link transmembrane receptors to the actin cytoskeleton [19]. The actin cytoskeleton is an essential structural and functional element that controls cell shape, cell motility and adhesion. When the extracellular environment is altered, these structures are disassembled and remodeled

to meet the new requirements [12]. To examine whether Tns2 is involved in adhesion and migration in podocytes, MPC5 cells, a conditionally immortalized podocyte cell line, were transfected with siRNAs for the coding sequence of *Tns2,* and two assays were used to determine the effects of *Tns2* KD on adhesion and migration. Adhesion assays were performed to investigate the effect of *Tns2* KD on podocyte anchorage to the ECM. Reduced levels of Tns2 protein ideally should be verified by quantitative western blotting. However, because good Tns2 antibodies are not available, we used RT-qPCR to detect knockdown of *Tns2* mRNA. In KD cells, *Tns2* transcripts were significantly decreased compared to in control cells (Fig. 5A). We then examined the influence on adhesion to several types of ECM (collagen type IV, fibronectin, laminin and vitronectin). Figure 5B demonstrates that attachment of *Tns2*-KD podocytes did not differ from that of the negative control for any ECM. Thus, *Tns2* suppression does not significantly affect the adherence of podocytes under these conditions. The Tns paralog, Tns1, has also been demonstrated to interact with and regulate the actin cytoskeleton or integrin [5].

To observe actin reorganization, we created wound gaps in cell monolayers by scratching a straight line with a 200-μl tip. *Tns2* KD produced a tendency toward increased migration in the scratch assay (data not shown). We monitored the actin architecture in *Tns2* KD podocytes migrating towards the center of the gap by staining with conjugated phalloidin-Alexa Fluor 594 (Fig. 5C). The degree of actin stress fiber formation was classified into three categories (high to low: a, b and c), depending on the thickness and length of the actin stress fibers in the cytoplasm. In *Tns2*-KD podocytes,
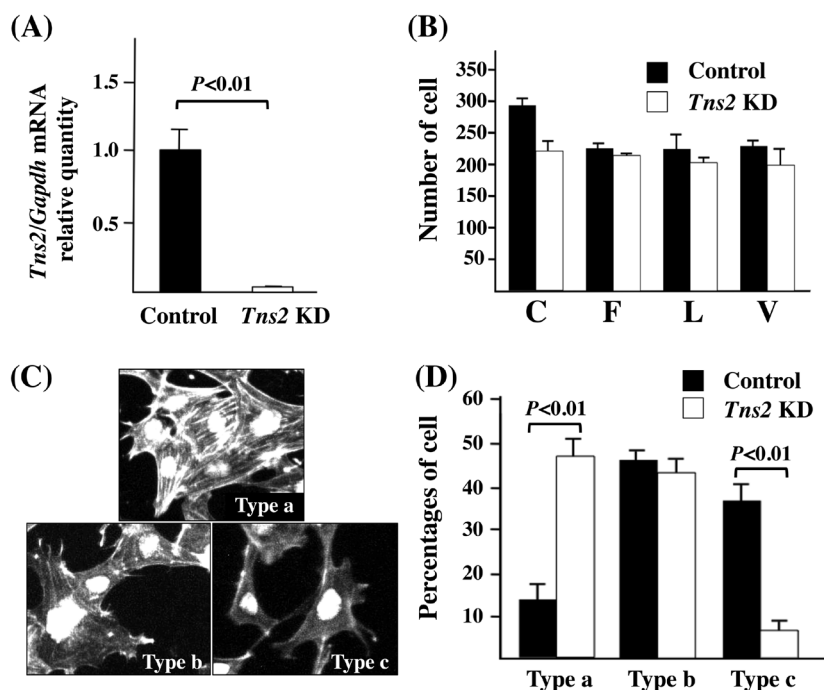
(A)

(B)

(C)

(D)

Fig. 5. Decreased *Tns2* mRNA expression results in increased formation of actin stress fibers. (A) Real-time PCR analysis of *Tns2* mRNA. Three days after siRNA transfection, *Tns2* mRNA expression significantly decreased in *Tns2* KD cells (n=3). (B) Adhesion assay of *Tns2* KD cells. Cells were seeded on culture dishes coated with collagen type IV (C), fibronectin (F), laminin (L) or vitronectin (V). After incubation for 1 hr, non-adherent cells were removed by gentle washing with PBS and then counted (n=3). (C)–(D) Quantification of phalloidin staining in *Tns2* KD cells. The degree of actin stress fiber formation was classified into three categories (high to low: a, b and c), depending on the thickness and length of the actin stress fibers in the cytoplasm. In *Tns2* KD podocytes, cells in the stress fiber-rich category, with thick cables, (type a) increased, whereas cells lacking stress fibers, without thick cables, (type c) decreased, suggesting that *Tns2* suppression significantly enhanced actin stress fiber formation (Fig. 5C and 5D). *Tns2*-KD podocytes were compared with control cells in 5 separate fields (n=5).

cells in category a (rich in stress fibers, with thick cables) increased, but the number of those in category b was similar to control cells. In contrast, cells in category c (with few stress fibers) decreased, suggesting that *Tns2* suppression significantly enhanced actin stress fiber formation (Fig. 5C and 5D). Next, to quantify cell migration accurately, we performed a transwell migration assay, which is widely used for studying the motility of different types of cells. Cells that migrated across the transwell membrane were quantified by fixing and counting. In general, migrating cells have thicker stress fibers than non-motile cells. As expected, *Tns2* KD in the podocyte cell line significantly enhanced cell migration (Fig. 6A and 6B).

DISCUSSION

In this study, to test whether *Tns2^nph^* might cause the mutant phenotype, we crossed *nph/nph* mice with mice that carried a SH2-PTB domain deletion. Compound heterozygotes that inherited both *Tns2^nph^* and *Tns2^ΔC^* displayed marked GS and proteinuria, indicating that these two mutations are allelic, and confirming that Tns2 deficiency is responsible for the GS phenotype. Further, KD of *Tns2* expression in the podocyte cell line increased both actin stress fiber forma-

tion and migration speed. There are several basic types of proteinuria, including glomerular, tubular, overflow and exercise-induced proteinuria. Glomerular proteinuria accounts for approximately 90% of all proteinuria [24]. Proteinuria arises due to injury of the glomerular filtration barrier. The currently available evidence suggests that podocytes act as the main component of this barrier, as mutations in a number of podocyte-specific genes have been identified to be responsible for GS [23, 36]. Thus, podocyte dysfunction is a common determining factor for progression toward many types of kidney diseases. A study of several inherited diseases in humans and of KO mouse models revealed that mutations in several podocyte genes (*ACTN4*, *CD2AP*, *SYNPO*, *MYH9*, *ARHGDIA* and *ARHGAP24*) lead to GS [1, 7, 9, 15–17]. These proteins are involved in actin organization in podocytes and the mutations results in FP effacement. Thus, it has become ever clearer that the precise organization and regulation of the actin cytoskeleton in podocytes is essential for the maintenance of normal structure and function and the actin cytoskeleton serves as the common final pathway organizing FP effacement, independent of the cause of podocyte damage [12, 22].

The function of Tns2 can be predicted based on its interactions with proteins of known function. Tensins are a
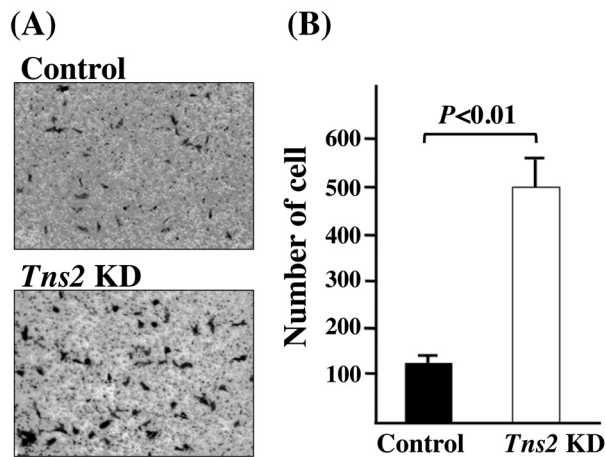
(A)

Control

Tns2 KD

(B)

Fig. 6.   Decreased *Tns2* mRNA expression results in increased cell migration. Transwell assay of *Tns2*-KD and control cells. Cells were seeded on the upper side of the inserts. After incubation for 24 hr, migrated cells were fixed and stained with crystal violet and then quantified by counting the number of cells in each well (n=3). Representative images of the migration of control and *Tns2* KD cells. Magnification, ×200. The number of migrated cells was counted in each group. In *Tns2*-KD podocytes, the number of migrating cells significantly increased.

family of proteins that are localized to integrin-linked focal adhesions. Four members have been identified: Tns1, Tns2, Tns3 and Tns4 [19]. All isoforms contain a PTB that allows them to interact with the cytoplasmic tail of β integrin. The N-terminal region of Tns1 interacts with actin at multiple sites, thereby linking the actin cytoskeleton to β integrin [11]. Both α3 integrin- and β1 integrin-KO mice show podocyte abnormalities and proteinuria similar to that of Tns2-deficient mutants [31]. Although no *Tns2* mutation has been found to be associated with human disease, expression of *TNS2* and *TNS3* at the mRNA and protein levels was found to be largely absent in a panel of diverse human cancer cell lines [21]. The loss of Tns3 leads to greater tumor cell motility and consequent metastasis, similar to our *in vitro* results [21]. Thus, it appears that Tns2 might anchor integrins to the cytoskeleton or integrins to the ECM, rendering podocytes stable. In contrast, deleted in liver cancer 1 (DLC1) is a recently identified tumor suppressor gene that is frequently underexpressed in hepatocellular carcinomas (HCCs). DLC1 encodes a Rho GTPase-activating protein domain that exhibits growth-suppressive activity in HCC cell lines [38]. Through its RhoGAP domain, DLC1 inhibits the activity of RhoA GTPase, which regulates the actin cytoskeleton network [34]. It has been reported that the Tns2 SH2-PTB domain binds to the DLC1 protein. Human DLC1 and TNS2 interact and co-localize to punctate structures at focal adhesions, and their interaction is required for tumor suppressive function [4]. In addition, *Dlc1* KD or KO increases actin stress fiber formation, similar to our result for *Tns2* KD [2, 37]. Since *Dlc1*-KO embryos did not survive beyond 10.5 days post coitum [8], it is unclear whether DLC1 is essential to maintain podocyte viability and function. The mouse

podocyte mRNA expression database contains mRNA expression data from FACS-sorted mouse podocytes, as analyzed by RNA sequencing [18]. This database shows that both *Tns2* and *Dlc1* mRNA are highly expressed in podocytes. These results suggest that both proteins may play roles in the regulation of actin reorganization in podocytes. Our *Tns2^{ΔC}* mice will contribute to determination of which of the Tns2-integrin and the Tns2-DLC1 signaling axes is essential for the precise organization and regulation of the actin cytoskeleton in podocytes.

In conclusion, we show here that Tns2 regulates the podocyte cytoskeleton. Further analysis of Tns2 should provide a better understanding of the molecular mechanisms of podocyte cytoskeleton regulation. Moreover, these studies may lead to the development of podocyte-specific drugs for restoration of the actin cytoskeleton in podocytes.

REFERENCES

1. Akilesh, S., Suleiman, H., Yu, H., Stander, M. C., Lavin, P., Gbadegesin, R., Antignac, C., Pollak, M., Kopp, J. B., Winn, M. P. and Shaw, A. S. 2011. Arhgap24 inactivates Rac1 in mouse podocytes, and a mutant form is associated with familial focal segmental glomerulosclerosis. *J. Clin. Invest.* **121**: 4127–4137. [Medline] [CrossRef]
2. Basak, P., Dillon, R., Leslie, H., Raouf, A. and Mowat, M. R. 2015. The Deleted in Liver Cancer 1 (Dlc1) tumor suppressor is haploinsufficient for mammary gland development and epithelial cell polarity. *BMC Cancer* **15**: 630. [Medline] [CrossRef]
3. Calderwood, D. A., Fujioka, Y., de Pereda, J. M., García-Alvarez, B., Nakamoto, T., Margolis, B., McGlade, C. J., Liddington, R. C. and Ginsberg, M. H. 2003. Integrin beta cytoplasmic domain interactions with phosphotyrosine-binding domains: a structural prototype for diversity in integrin signaling. *Proc. Natl. Acad. Sci. U.S.A.* **100**: 2272–2277. [Medline] [CrossRef]
4. Chan, L. K., Ko, F. C., Ng, I. O. and Yam, J. W. 2009. Deleted in liver cancer (DLC1) utilizes a novel binding site for Tensin2 PTB domain interaction and is required for tumor-suppressive function. *PLOS ONE* **4**: e5572. [Medline] [CrossRef]
5. Chen, H. and Lo, S. H. 2003. Regulation of tensin-promoted cell migration by its focal adhesion binding and Src homology domain 2. *Biochem. J.* **370**: 1039–1045. [Medline] [CrossRef]
6. Cho, A. R., Uchio-Yamada, K., Torigai, T., Miyamoto, T., Miyoshi, I., Matsuda, J., Kurosawa, T., Kon, Y., Asano, A., Sasaki, N. and Agui, T. 2006. Deficiency of the tensin2 gene in the ICGN mouse: an animal model for congenital nephrotic syndrome. *Mamm. Genome* **17**: 407–416. [Medline] [CrossRef]
7. Deller, T., Korte, M., Chabanis, S., Drakew, A., Schwegler, H., Stefani, G. G., Zuniga, A., Schwarz, K., Bonhoeffer, T., Zeller, R., Frotscher, M. and Mundel, P. 2003. Synaptopodin-deficient mice lack a spine apparatus and show deficits in synaptic plasticity. *Proc. Natl. Acad. Sci. U.S.A.* **100**: 10494–10499. [Medline] [CrossRef]

8. Durkin, M. E., Avner, M. R., Huh, C. G., Yuan, B. Z., Thorgeirsson, S. S. and Popescu, N. C. 2005. DLC-1, a Rho GTPase-activating protein with tumor suppressor function, is essential for embryonic development. *FEBS Lett.* **579**: 1191–1196. [Medline] [CrossRef]

9. Gee, H. Y., Saisawat, P., Ashraf, S., Hurd, T. W., Vega-Warner, V., Fang, H., Beck, B. B., Gribouval, O., Zhou, W., Diaz, K. A., Natarajan, S., Wiggins, R. C., Lovric, S., Chernin, G., Schoeb, D. S., Ovunc, B., Frishberg, Y., Soliman, N. A., Fathy, H. M., Goebel, H., Hoefele, J., Weber, L. T., Innis, J. W., Faul, C., Han, Z., Washburn, J., Antignac, C., Levy, S., Otto, E. A. and Hildebrandt, F. 2013. ARHGDIA mutations cause nephrotic syndrome via defective RHO GTPase signaling. *J. Clin. Invest.* **123**: 3243–3253. [Medline] [CrossRef]

10. Grenz, H., Carbonetto, S. and Goodman, S. L. 1993. Alpha 3 beta 1 integrin is moved into focal contacts in kidney mesangial cells. *J. Cell Sci.* **105**: 739–751. [Medline]

11. Haynie, D. T. 2014. Molecular physiology of the tensin brotherhood of integrin adaptor proteins. *Proteins* **82**: 1113–1127. [Medline] [CrossRef]

12. He, F. F., Chen, S., Su, H., Meng, X. F. and Zhang, C. 2013. Actin-associated proteins in the pathogenesis of podocyte injury. *Curr. Genomics* **14**: 477–484. [Medline] [CrossRef]

13. Jin, X., Wang, W., Mao, J., Shen, H., Fu, H., Wang, X., Gu, W., Liu, A., Yu, H., Shu, Q. and Du, L. 2014. Overexpression of Myo1e in mouse podocytes enhances cellular endocytosis, migration, and adhesion. *J. Cell. Biochem.* **115**: 410–419. [Medline] [CrossRef]

14. Jinek, M., Chylinski, K., Fonfara, I., Hauer, M., Doudna, J. A. and Charpentier, E. 2012. A programmable dual-RNA-guided DNA endonuclease in adaptive bacterial immunity. *Science* **337**: 816–821. [Medline] [CrossRef]

15. Kaplan, J. M., Kim, S. H., North, K. N., Rennke, H., Correia, L. A., Tong, H. Q., Mathis, B. J., Rodríguez-Pérez, J. C., Allen, P. G., Beggs, A. H. and Pollak, M. R. 2000. Mutations in ACTN4, encoding alpha-actinin-4, cause familial focal segmental glomerulosclerosis. *Nat. Genet.* **24**: 251–256. [Medline] [CrossRef]

16. Kelley, M. J., Jawien, W., Ortel, T. L. and Korczak, J. F. 2000. Mutation of MYH9, encoding non-muscle myosin heavy chain A, in May-Hegglin anomaly. *Nat. Genet.* **26**: 106–108. [Medline] [CrossRef]

17. Kim, J. M., Wu, H., Green, G., Winkler, C. A., Kopp, J. B., Miner, J. H., Unanue, E. R. and Shaw, A. S. 2003. CD2-associated protein haploinsufficiency is linked to glomerular disease susceptibility. *Science* **300**: 1298–1300. [Medline] [CrossRef]

18. Knepper, M. A. Podocyte Transcriptome. Available at https://hpcwebapps.cit.nih.gov/ESBL/Database/Podocyte_Transcriptome/index.htm (Accessed 2 May 2016).

19. Lo, S. H. 2004. Tensin. *Int. J. Biochem. Cell Biol.* **36**: 31–34. [Medline] [CrossRef]

20. Mali, P., Esvelt, K. M. and Church, G. M. 2013. Cas9 as a versatile tool for engineering biology. *Nat. Methods* **10**: 957–963. [Medline] [CrossRef]

21. Martuszewska, D., Ljungberg, B., Johansson, M., Landberg, G., Oslakovic, C., Dahlbäck, B. and Hafizi, S. 2009. Tensin3 is a negative regulator of cell migration and all four Tensin family members are downregulated in human kidney cancer. *PLOS ONE* **4**: e4350. [Medline] [CrossRef]

22. Mathieson, P. W. 2012. The podocyte cytoskeleton in health and in disease. *Clin. Kidney J.* **5**: 498–501. [Medline] [CrossRef]

23. Mundel, P., Schwarz, K. and Reiser, J. 2001. Podocyte biology: a footstep further. *Adv. Nephrol. Necker Hosp.* **31**: 235–241. [Medline]

24. Mundel, P. and Reiser, J. 2010. Proteinuria: an enzymatic disease of the podocyte? *Kidney Int.* **77**: 571–580. [Medline] [CrossRef]

25. Mundel, P., Reiser, J., Zúñiga Mejía Borja, A., Pavenstädt, H., Davidson, G. R., Kriz, W. and Zeller, R. 1997. Rearrangements of the cytoskeleton and cell contacts induce process formation during differentiation of conditionally immortalized mouse podocyte cell lines. *Exp. Cell Res.* **236**: 248–258. [Medline] [CrossRef]

26. Nishino, T., Sasaki, N., Chihara, M., Nagasaki, K., Torigoe, D., Kon, Y. and Agui, T. 2012. Distinct distribution of the tensin family in the mouse kidney and small intestine. *Exp. Anim.* **61**: 525–532. [Medline] [CrossRef]

27. Nitta, T., Muro, R., Shimizu, Y., Nitta, S., Oda, H., Ohte, Y., Goto, M., Yanobu-Takanashi, R., Narita, T., Takayanagi, H., Yasuda, H., Okamura, T., Murata, S. and Suzuki, H. 2015. The thymic cortical epithelium determines the TCR repertoire of IL-17-producing γδT cells. *EMBO Rep.* **16**: 638–653. [Medline] [CrossRef]

28. Ogura, A., Asano, T., Matsuda, J. and Fujimura, H. 1991. Evolution of glomerular lesions in nephrotic ICGN mice: serial biopsy study with electron microscopy. *J. Vet. Med. Sci.* **53**: 513–515. [Medline] [CrossRef]

29. Ogura, A., Asano, T., Matsuda, J., Takano, K., Nakagawa, M. and Fukui, M. 1989. Characteristics of mutant mice (ICGN) with spontaneous renal lesions: a new model for human nephrotic syndrome. *Lab. Anim.* **23**: 169–174. [Medline] [CrossRef]

30. Pavenstädt, H., Kriz, W. and Kretzler, M. 2003. Cell biology of the glomerular podocyte. *Physiol. Rev.* **83**: 253–307. [Medline] [CrossRef]

31. Pozzi, A., Jarad, G., Moeckel, G. W., Coffa, S., Zhang, X., Gewin, L., Eremina, V., Hudson, B. G., Borza, D. B., Harris, R. C., Holzman, L. B., Phillips, C. L., Fassler, R., Quaggin, S. E., Miner, J. H. and Zent, R. 2008. Beta1 integrin expression by podocytes is required to maintain glomerular structural integrity. *Dev. Biol.* **316**: 288–301. [Medline] [CrossRef]

32. Sasaki, H., Sasaki, N., Nishino, T., Nagasaki, K., Kitamura, H., Torigoe, D. and Agui, T. 2014. Quantitative trait loci for resistance to the congenital nephropathy in tensin 2-deficient mice. *PLOS ONE* **9**: e99602.

33. Sasaki, H., Marusugi, K., Kimura, J., Kitamura, H., Nagasaki, K., Torigoe, D., Agui, T. and Sasaki, N. 2015. Genetic background-dependent diversity in renal failure caused by the tensin2 gene deficiency in the mouse. *Biomed. Res.* **36**: 323–330. [Medline] [CrossRef]

34. Shih, Y. P., Sun, P., Wang, A. and Lo, S. H. 2015. Tensin1 positively regulates RhoA activity through its interaction with DLC1. *Biochim. Biophys. Acta* **1853**: 3258–3265. [Medline] [CrossRef]

35. Uchio-Yamada, K., Sawada, K., Tamura, K., Katayama, S., Monobe, Y., Yamamoto, Y., Ogura, A. and Manabe, N. 2013. Tenc1-deficient mice develop glomerular disease in a strain-specific manner. *Nephron, Exp. Nephrol.* **123**: 22–33. [Medline] [CrossRef]

36. Wiggins, R. C. 2007. The spectrum of podocytopathies: a unifying view of glomerular diseases. *Kidney Int.* **71**: 1205–1214. [Medline] [CrossRef]

37. Xue, W., Krasnitz, A., Lucito, R., Sordella, R., Vanaelst, L., Cordon-Cardo, C., Singer, S., Kuehnel, F., Wigler, M., Powers, S., Zender, L. and Lowe, S. W. 2008. DLC1 is a chromosome 8p tumor suppressor whose loss promotes hepatocellular carcinoma. *Genes Dev.* **22**: 1439–1444. [Medline] [CrossRef]

38. Yam, J. W., Ko, F. C., Chan, C. Y., Jin, D. Y. and Ng, I. O. 2006. Interaction of deleted in liver cancer 1 with tensin2 in caveolae and implications in tumor suppression. *Cancer Res.* **66**: 8367–8372. [Medline] [CrossRef]